Fractal dimension of lightning discharge

J. Sañudo, J. B. Gómez, F. Castaño, A. F. Pacheco

Nonlinear Processes in Geophysics (1995) 2: 101 - 106

Nonlinear Processes in Geophysics

Fractal dimension of lightning discharge

J. Sañudo[1], J. B. Gómez[2], F. Castaño[1] and A. F. Pacheco[3]

[1] Departamento de Física, Facultad de Ciencias, Universidad de Extremadura, 06071 Badajoz, Spain
[2] Department of Geological Sciences, University College London, Gower St., London WC1 6BT, U.K.
[3] Departamento de Física Teórica, Universidad de Zaragoza, 50009 Zaragoza, Spain

Received 25 July 1994 - Accepted 9 March 1995 - Communicated by D. Schertzer

Abstract. Using a stochastic model, we simulate the process of dielectric breakdown in the atmosphere and calculate the fractal dimension of 3-dimensional lightning patterns. Finite-size effects have been studied. The projections of our patterns on vertical planes fit the experimental fractal dimension obtained from photographic analysis. This work is inspired by a previous work by A.A. Tsonis.

1 Introduction

In this paper we apply the stochastic dielectric breakdown (DB) model (Niemeyer et al., 1984) to describe the geometric structure of lightning discharge in the atmosphere. As is known, the branched structure of lightning is due to the zig-zag progress of the stepped leader searching for the most favourable (weakest) path from a cloud to the ground (or *vice versa*). This branched ionized channel is strongly illuminated almost immediately during the return stroke, allowing a plot of the luminous image to be obtained. For details the reader is referred to, for example, Uman (1969, and 1987) or to Houghton (1985). In a first paper on this subject, Tsonis and Elsner (1987) and Tsonis (1991) analyzed a set of lightning photographs (Salanave, 1980) and deduced that the average fractal dimension of the lightning images is $\bar{D}_p \simeq 1.34 \pm 0.05$.(Note that we use the subscript p to emphasize that it refers to a projected image). With this observation, flashes of lightning entered into the already wide subject of applications of fractals to natural phenomena, (Mandelbrot,1983). Then, Tsonis (1991) built a simple DB model in 2 dimensions in order to reproduce the quantitative fractal behaviour observed in the photographs.

As mentioned above, the stochastic DB model, its relation to the physics of dielectric breakdown in gases (Meek and Graggs, 1978), and its relation to the Diffusion Limited Aggregation schemes has been developed by Niemeyer et al. (1984). See also the references contained in Pietronero and Tosatti (Eds.) (1988). In the DB model one plays with a parameter, η, which fixes the dependence of the growth probability on the local electric field. For a discussion on this parameter see Pietronero and Wiesmann (1988). As a lightning discharge is actually a 3-dimensional (3D thereafter) phenomenon, here we apply a DB model, *a la* Tsonis, but building 3D simulations of lightning patterns. We conclude that the value $\bar{D}_p \simeq 1.34$ observed in photos of lightning implies a much bigger value for η, than that deduced in the previous 2D calculations.

The structure of this paper is as follows. In Section 2 we give the details of how to simulate the lightning patterns. Section 3 is devoted to the presentation and discussion of the results obtained for the average 3D fractal dimension, $\bar{D}$, as well as the average fractal dimension of the vertical projection, $\bar{D}_p$. All these results are obtained as a function of η. The importance of finite-size effects is also tested. Finally in Section 4 we state our conclusions, and make a short critical discussion.

2 3-Dimensional Dielectric Breakdown Model

As mentioned, the method followed here to build the spatial structure of a lightning discharge is based on the stochastic fractal model proposed by Niemeyer et al. (1984) to simulate the dielectric breakdown in gases. We build lightning patterns confined in a parallelepipedic box, Fig. 1, with electrostatic potential $\phi = 0$ in the upper face (which simulates the cloud base) and $\phi = 1$ in the lower face (which simulates the ground). With regards to the lateral faces of the box we assume, with Tsonis (1991), that ϕ verifies there periodic boundary conditions. The volume contained within the box is discretized into a $60 \times 100 \times 100$ cubic lattice. Only the central site of the top face (A1 in Fig. 1), is assumed to be able to initiate the discharge. With the mentioned

Correspondence to: A. F. Pacheco

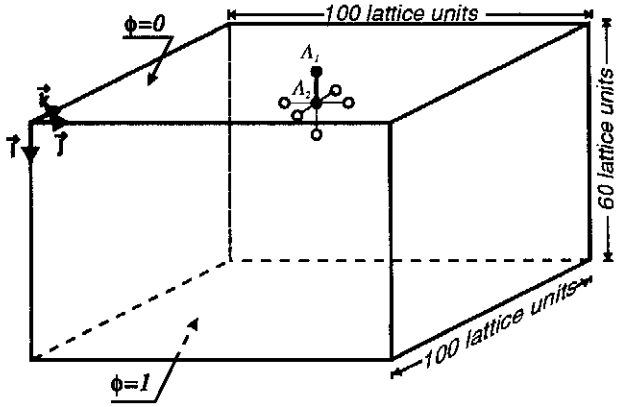

Fig. 1. 3D model used to simulate lightning discharge. The point A_1 marks the start of the electric breakdown, which extends to the black circle A_2; the broken site is linked by a thick solid line. The open circles indicate the possible subsequent growth sites.

boundary conditions, the electric potential at any point of the lattice fulfils Laplace's equation $\nabla^2\phi = 0$. On a 3D lattice, this condition is enforced by iterating until we obtain convergent results in the equation:

$$\begin{aligned}\phi(i,j,k) &= \frac{1}{6}[\phi(i+1,j,k)+\phi(i-1,j,k)+ \\ &\quad \phi(i,j+1,k)+\phi(i,j-1,k)+ \\ &\quad \phi(i,j,k+1)+\phi(i,j,k-1)]. \end{aligned} \tag{1}$$

Once the value of ϕ is known everywhere in the box (that is, in all the sites of the lattice), all the nearest neighbours to the point A1 are then considered as possible candidates to continue the discharge and one of them will eventually be added to the growing lightning pattern. In Fig. 1, the candidates are indicated by open circles and the existing pattern by black lines joining black circles. In step 1 there is only 1 candidate. Thus, point A2 is directly added to the pattern, and hence A2 forms part of the $\phi = 0$ equipotential region. In step 2 one again solves Laplace's equation on the lattice using the new pattern as a new boundary condition. The number of possible candidate sites in step 2 is five and each of them is assumed to have the probability of being added to the growing cluster indicated by the equation

$$P_i = \frac{\phi_i^\eta}{\sum_{i=1}^n \phi_i^\eta} \qquad (i = 1, ..., n), \tag{2}$$

where n is the number of candidate sites in each step; in this case $n = 5$. [According to Eq. 2, η parametrizes the relation existing between the local electric field and the probability of dielectric breaking in that site]. In this form, at each step of the growing process a probability distribution is defined for the set of candidate sites. Then, one point is randomly selected and added to the pattern. This procedure is repeated until the lightning pattern descends to the ground plane.

From the technical point of view, the iteration until convergence of Eq. 1 is the most demanding part of the whole process. If one uses standard relaxation techniques, a more convenient form for Eq. 1 is the following (Carnahan et al., 1977):

$$\begin{aligned}\phi(i,j,k) &= \phi(i,j,k)+ \\ &\quad \frac{w}{6}[\phi(i+1,j,k)+\phi(i-1,j,k)+ \\ &\quad \phi(i,j+1,k)+\phi(i,j-1,k)+ \\ &\quad \phi(i,j,k+1)+\phi(i,j,k-1)- \\ &\quad 6\phi(i,j,k)], \end{aligned} \tag{3}$$

where w plays the role of a convergence parameter. For $w = 1$, we recover Eq. 1. We have numerically checked that $w \simeq 1.6$ increases considerably the speed of convergence of the whole process, and about 15 iterations are enough, on an average, to reduce the relative error to less than 0.001. In contrast, with $w = 1$ the number of necessary iterations doubles or even triples. We should add in this respect that the use of the w parameter not only speeds up the process of convergence but also reduces the final global error. As said before, when a new point is added to the growing pattern, Laplace's equation has to be solved with the new boundary condition. To speed up this process even more, we have used a second computational trick consisting in solving first Eq. 3 for the sites of a 6×6×6 cube centred in the new added point. Once the 0.1% convergence criterion is reached for this subsystem (this takes, say, 15 iterations), we proceed to solve the total system. The convergence now typically demands 5 steps for $\eta = 2$ and 10 steps for $\eta = 9$. The obvious reason for using this additional trick is that the changes in ϕ, after the addition of a new point to the pattern, are particularly strong in the surrounding of the new added point, whilst the effect declines quickly with distance.

Eq. 2 also deserves a comment. When one performs the sum in the denominator to normalize the respective probabilities, one should be careful to avoid rounding errors. This can be avoided by summing up the various terms in ascending order. If this is not taken into account, the introduced errors are large even in the case of small η's.

To give an impression of the CPU times involved in these simulations, we will mention that each simulation, for $\eta = 2$, of patterns involving from about 900 to 1600 points takes between 5.5 and 10 hours of CPU on a CONVEX C210 computer. Whereas patterns of 120 points, for $\eta = 9$, take about 1 hour of CPU time.

There are several standard ways of estimating the Haussdorf dimension of a fractal pattern. Here we have chosen the radius of gyration, R_g, method by computing

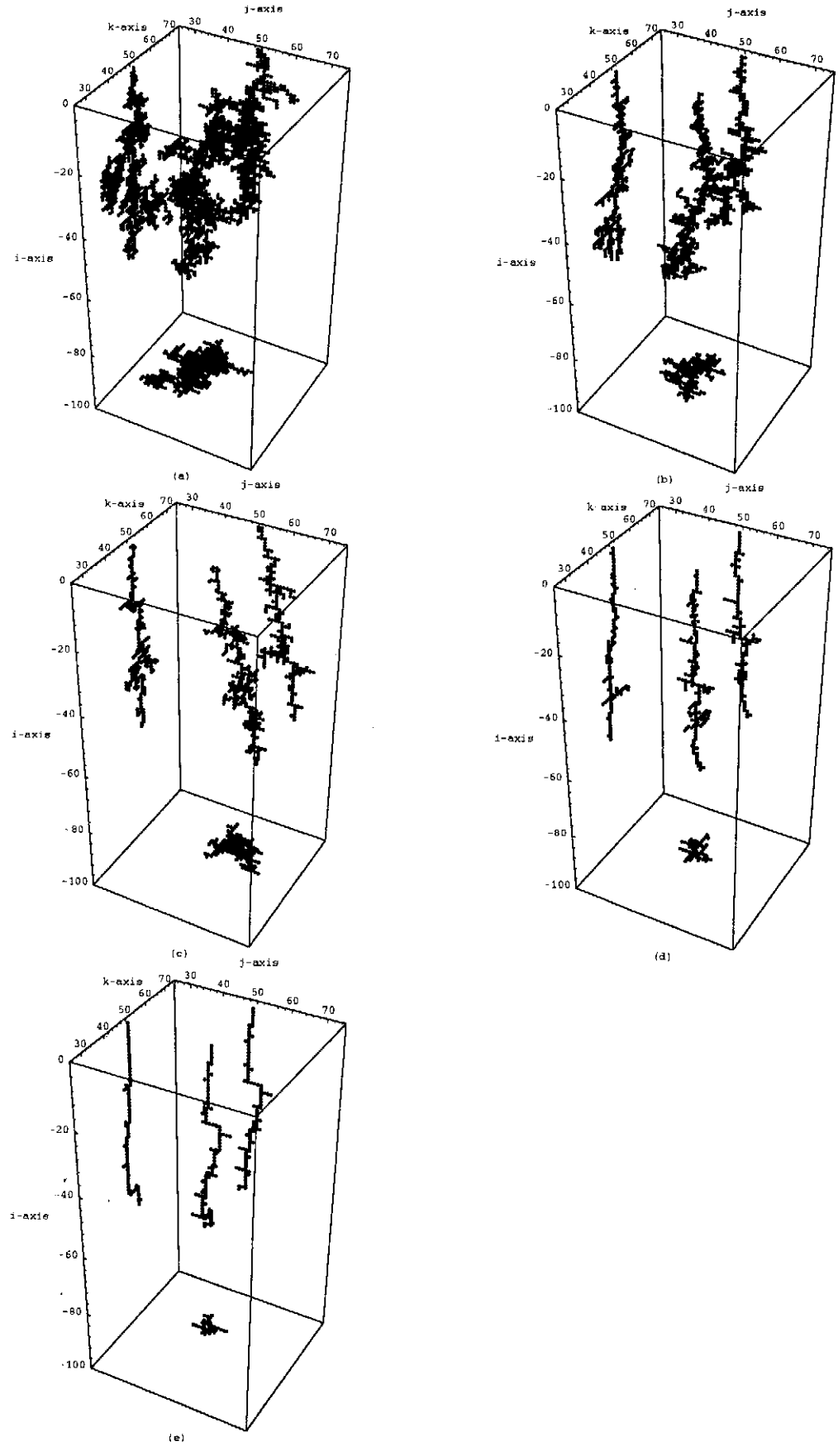

Fig. 2. Examples of simulated lightning patterns and their plane projections. (a) $\eta = 2$, (b) $\eta = 3$, (c) $\eta = 4$, (d) $\eta = 6$, (e) $\eta = 9$. To clarify the figure the black lines that link the open circles have been suppressed.

Table 1. Hausdorff dimensions of simulated lightning patterns for different η values.

a	60x100x100 lattice				
	$\eta = 2$	$\eta = 3$	$\eta = 4$	$\eta = 6$	$\eta = 9$
$\bar{D}$	2.17 ± 0.04	1.90 ± 0.03	1.73 ± 0.03	1.51 ± 0.02	1.34 ± 0.02
$\bar{N}$	1193 ± 48	511 ± 21	336 ± 22	184 ± 6	117 ± 2
N_s	21	22	26	30	30
b	30x50x50 lattice				
$\bar{D}$	2.20 ± 0.04	1.89 ± 0.04	1.77 ± 0.04	1.49 ± 0.03	1.30 ± 0.02
$\bar{N}$	325 ± 12	142 ± 9	105 ± 4	64 ± 2	46 ± 1
N_s	22	23	28	30	31

Table 2. Hausdorff dimensions of lightning projections onto the (i,j) or (i,k) planes.

a	60x100x100 lattice				
	$\eta = 2$	$\eta = 3$	$\eta = 4$	$\eta = 6$	$\eta = 9$
$\bar{D}_p$	1.88 ± 0.02	1.69 ± 0.02	1.54 ± 0.02	1.34 ± 0.01	1.21 ± 0.01
$\bar{N}_p$	500 ± 12	263 ± 8	186 ± 4	123 ± 2	89 ± 1
b	30x50x50 lattice				
$\bar{D}$	1.85 ± 0.02	1.63 ± 0.02	1.54 ± 0.03	1.29 ± 0.01	1.17 ± 0.01
$\bar{N}$	154 ± 3	87 ± 2	67 ± 2	47 ± 1	38 ± 1

the slope of a linear fit to a plot of $\ln R_g$ vs $\ln N(r)$, during the growth process of the pattern. $R_g = [\sum_{i \neq j}(r_i - r_j)^2]^{1/2}$ is a measure of the size of the growing cluster. r_j is the position vector of each point in the pattern, and $N(r)$ is the number of points belonging to the pattern, contained within a sphere of radius r, with origin at the centre of mass. For a fractal cluster, the radius of gyration fulfils

$$R_g \propto N^{\beta}. \tag{4}$$

The exponent β is related to the Haussdorf dimension, D, by the relation $D = 1/\beta$. The fractal dimension has been estimated by a straight line fit of the radius of gyration-curve (a ln-ln plot), the slope of which provides the fractal dimension sought.

3 Results

The averaged fractal dimension, $\bar{D}$, for 5 different η values of our computer-generated patterns is shown in Table 1a. In the table we can see the average size of the patterns, $\bar{N}$, and the number of performed simulations, N_s. The unavoidable errors appearing in the measurements are entirely due to the statistical handling of the data. In this table, one observes the decrease of $\bar{D}$ with η, which is quite natural because of the role of η in controlling the probability of growth.

To evaluate the impact that finite-size effects of our chosen lattice may have on the final results, we have performed a number of simulations in a "small" lattice of 30x50x50 sites. The results emerging from this smaller lattice are gathered in Table 1b. By comparing the figures of the two tables we conclude that the finite size effects induced in our final results are expected to be very small.

In Fig. 2 we have plotted several examples of 3D lightning patterns built for several values of η, together with the projections onto the (i,j),(i,k) and (j,k) planes. The criterion used to select these specific patterns has been that these figures have a fractal dimension close to the mean value, $\bar{D}$. The asymmetry between the vertical-plane projections and the horizontal-plane projections is as qualitatively expected.

The relevance of the projections on the vertical planes is based on the fact that the observation of the lightning structure is through photographs. Therefore, we have systematically performed the projections of the 3D lightning patterns and calculated the fractal dimension of the projected figures. At this point we must say that given a fractal set, its projection to a lower dimension may or may not be fractal. In this case our calculation support that the vertical projections of the 3D lightning pattern are indeed fractals. The average values of the projected fractal dimensions, $\bar{D}_p$, as a function of η, appear in Table 2a for the 60x100x100 lattice. The average value of the number of points on each plane, $\bar{N}_p$, is also included. The decrease of $\bar{D}_p$ with η has an explanation similar to that of the 3D case. To estimate the possible finite-size effects, we have also studied the value of $\bar{D}_p$ emerging from clusters grown in the smaller 30x50x50 lattice. These results are gathered in Table 2b. By comparing them with those of Table 2a, one concludes, as in the 3D case, that these effects are practically negligible.

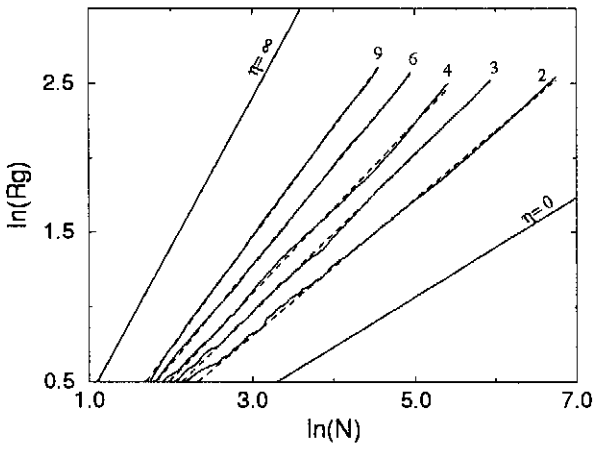

Fig. 3. Ln-ln plot of the average radius of gyration, R_g vs. average size, for patterns generated in a 60x100x100 lattice with η = 2, 3, 4, 6, and 9. The straight lines represent the best linear fit to the results. The cases with $\eta = 0$ and $\eta = \infty$ represent the two limiting situations for a 3D lattice.

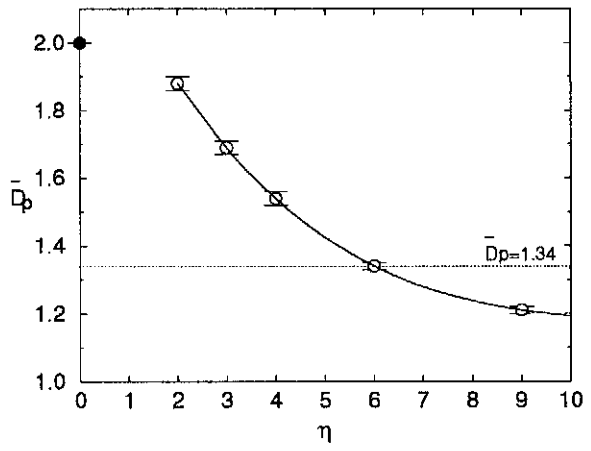

Fig. 4. Fractal dimension of the average lightning projections, $\bar{D}_p$, for the η values quoted in the text. The black dot,(•), represents what would be the Euclidean dimension. The dashed line corresponds to the value observed by Tsonis (1991) in lightning photos whereas the continuous line, obtained by polynomic interpolation, allows us to obtain graphically the fractal dimension for non-integer η values.

In Fig. 3, we have drawn for each η the average value of the radius of gyration of all the simulations and determined the best linear fit to these points. As is clear, the process of averaging considerably smoothes the behaviour of the individual results. Indeed, the average results do not differ much from the best linear fit.

The experimental (observational) value of $\bar{D}_p$ according to Tsonis (1991) is $\bar{D}_p \simeq 1.34$. In Fig. 4, we have plotted the $\bar{D}_p$ values obtained in this study as a function of η. $\bar{D}_p \simeq 1.34$ is obtained precisely for $\eta = 6$; this corresponds to a 3D fractal dimension of $\bar{D} \simeq 1.51$.

4 Discussion and Conclusions

In this paper we have simulated the structure of lightning discharges using the η (or DB) model. We have carried out a 3D analysis in volumes comprising 6×10^5 lattice sites, and projecting the resulting 3D patterns onto vertical planes in order to make a proper comparison with photographs of real lightning. The agreement between our model and the photos occurs for a value of $\eta \simeq 6$ which is significantly different from the value obtained by Tsonis (1991) in his 2D calculations. The finite-size effects have been tested by comparing these results with the patterns calculated, with the same working rules, in volumes of 30x50x50 lattice sites. This comparison indicates that finite-size effects are actually negligible.

Our results for the fractal dimension of lightning indicates that a 3D pattern with $\bar{D} \simeq 1.51$ has a plane projection of $\bar{D}_p \simeq 1.34$ which is the value observed in the photos. Our finding of $\eta \simeq 6$ as the phenomenological correct value of this parameter implies that lightning structure is considerably more deterministic than what the $\eta = 2$ value implied. In our opinion, to find a quantitative argument of why the 2D simulations by Tsonis (1991) with $\eta = 2$ have the same fractal dimension as the projections of our 3D patterns with $\eta = 6$ is not an easy task because that would require an analytic relation between η and $\bar{D}$, which is not known. However, it is rather intuitive to foresee an increase in η just thinking in the additional horizontal direction available for the lightning pattern to grow.

As mentioned in the introductory paragraphs, the microscopic physical foundations of the stochastic DB model, when applied to gas discharges, has been discussed by Pietronero and Wiesmann (1988) and references therein. Certainly, the theory of all the processes occurring in real lightnings discharges is understood in a general way but many details remain yet uncertain, and even controversial. In spite of their unquestionable similarities, a lightning discharge is by far a much more complex phenomenon than any spark provoked in the lab. It is believed that the stepped leader starts at the dielectric breakdown of water drops elongated by particularly high electric fields in certain regions of the clouds. Once initiated, the discharge propagates in a process of an electron avalanche fed by successive ionizations. In its progress downwards, the leader finds a number of inhomogeneities related to air and ion densities, water content, etc. The leader propagation velocity is of the order of $1.5 \times 10^5 \mathrm{ms}^{-1}$, the length of a leader step is about 50 m, and the time interval between steps is about 50 μs.

Thus, the DB model used in this paper which has no more inputs than a simplified electrostatics and a constant rule to relate local electric field to growth probability, is obviously a very schematic representation of reality. For example no reference to electrodynamics is

made, no finite critical fields have been taken into account (Wiesmann,1989), and the calculations have been performed without worrying about what would be the actual length of the lattice step used in the model, or the potential-drop evolution in the process. In lightning there are many obvious sources of stochasticity in the propagation of stepped leaders, but it is not easy to make an accurate identification between them and the value of the η parameter here found. Our result, $\eta \simeq 6$, might however be a useful guideline for future more detailed models.

Acknowledgements. We thank the criticism raised by the referees and A.A. Tsonis which has contributed to improve the content. One of the authors (AFP) thanks Björn Wolf and Angel Sanchez for useful comments and discussions. This work was supported by the Spanish DGICYT (PB93-0304). JBG is supported by a Spanish post-doctoral grant (PF93-25428779).

References

Carnahan, B., Luther, H.A., and Wilkes, J.O., *Applied Numerical Methods*, Wiley, 1977.

Houghton, H.G., *Physical meteorology*, MIT Press, Mass., 1985.

Mandelbrot, B., *The fractal geometry of nature*, Freeman, New York, 1983.

Meek, J.M.,and Craggs, J.D., *Electric breakdown in gases*, Wiley, 1987.

Niemeyer, L., Pietronero, L., and Wiesmann, H.J., Fractal dimension of dielectric breakdown, *Phys. Rev. Lett.*, *52*, 1033-1036, 1984.

Pietronero, L., and Tosatti, E.,(eds.), *Fractals in physics*, North Holland, 1986.

Pietronero, L., and Wiesmann, H.J., From physical dielectric breakdown to the stochastic fractal model, *Z. Phys.* B, *70*, 87-93, 1988.

Salanave, L.E., *Lightning and its spectrum*, University of Arizona Press, Arizona, 1980.

Tsonis, A.A., and Elsner, J.B., *Beitr. Phys. Atmos.*, *60*, 187-192, 1987.

Tsonis, A.A., A fractal study of dielectric breakdown in the atmosphere, In *Non Linear Variability in Geophysics*, 167-174, Schertzer, D., and Lovejoy, S. (Eds.), Kluwer, 1991.

Uman, M.A., *Lightning*, Mc Graw Hill, 1969.

Uman, M.A., *Lightning discharge*, Academic Press, 1987.

Wiesmann, H.J., Realistic models for dielectric breakdown, In *Fractals, Physical origin and Properties*, Pietronero, L., (Ed.), Plenum, New York, 1989.